JOURNAL OF GEOPHYSICAL RESEARCH, VOL. 101, NO. A6, PAGES 13,169–13,178, JUNE 1, 1996

Transfer of magnetosheath momentum and energy to the ionosphere along open field lines

Andrew N. Wright

Mathematical Institute, University of St. Andrews, Fife, Scotland

Abstract. A framework is established for describing the transfer of magnetosheath energy along open field lines to the ionosphere in terms of MHD (magnetohydrodynamic) waves. The evolution of field lines crossing an initial velocity shear is shown to extract momentum and energy from the faster flow (magnetosheath) and deposit it in the slower flow. If the slower plasma is taken to be at rest and have density ρ_0 and Alfvén speed V_A, while the faster plasma has flow speed V_0 and Alfvén speed V_A', then the rate of energy density exchange is $\rho_0 V_0^2 V_A^3/(V_A + V_A')^2$, while that of momentum density is $\rho_0 V_0 V_A^2/(V_A + V_A')$. The effect of an ionosphere is included by introducing a height-integrated Pedersen conductivity (Σ_p), and we find that field lines slip with a velocity $V_0/(1+\mu_0\Sigma_p V_A)$ just above the ionosphere. By considering the accelerated flows associated with newly opened field lines, it may be possible to understand transient features seen in data such as initial azimuthal surges.

1. Introduction

Data studies show that the opening of field lines (by reconnection) is frequently not done in a steady fashion but occurs in pulses [*Lockwood et al.*, 1995]. Such time-dependent behavior is described naturally in terms of MHD waves, which is the viewpoint developed here to complement "circuit analogy" studies [e.g., *Holzer and Reid*, 1975]. Indeed, *Maltsev et al.* [1977], *Southwood and Hughes* [1983], and *Hughes* [1983] all discussed magnetosphere-ionosphere coupling in terms of waves. For the most part these studies did not concern themselves with the magnetosheath and concentrated upon the effect of the ionosphere on the convection of closed magnetospheric flux tubes. For example, changes in ionospheric conductivity can launch Alfvén waves into the magnetosphere and modify the flows there. Here we reverse this philosopy and consider the effect of driven magnetospheric motion upon the ionosphere.

More recent studies have considered the effects of magnetospheric disturbances upon the ionosphere. For example, *Southwood* [1987] and *Glassmeier* [1992] discussed the ionospheric response to dayside reconnection and traveling convection vorticies. Generally, the physics is reduced to the reflection of magnetospheric MHD waves from a thin ionosphere [*Maltsev et al.*, 1977; *Newton et al.*, 1978; *Hughes*, 1983]. There have also been many studies of wave reflection from a nonuniform ionosphere, which may be applicable to the auroral zone [e.g., *Ellis and Southwood*, 1983; *Yarker and Southwood*, 1986; *Glassmeier*, 1988].

Paper number 96JA00541.
0148-0227/96/96JA-00541$09.00

Our approach has much in common with with studies that have addressed the development of magnetospheric flows driven by artificial [*Drell et al.*, 1965; *Scholer*, 1970] and natural [*Neubauer*, 1980; *Southwood et al.*, 1980; *Wright and Southwood*, 1987] satellites or other energy sources inside a magnetosphere [*Kan et al.*, 1982; *Glassmeier*, 1983; *Kan and Sun*, 1985]. Here we extend these concepts to include driving from outside the magnetosphere and treat open field lines more completely than earlier work. In particular, we present a novel description of magnetosheath-magnetosphere coupling in which the motion of magnetospheric flux tubes is described in terms of waves excited by the magnetosheath flow.

The paper is structured as follows: Section 2 presents a summary of basic concepts. Section 3 describes the extraction of energy from an idealized magnetosheath, while section 4 considers coupling to the ionosphere. Section 5 includes the possibility of accelerated flows resulting from reconnection. Section 6 discusses the ionospheric flows which may be excited, and section 7 concludes the paper.

2. Basic Concepts

In this section we review basic concepts from previous studies. To begin, with we consider the simple configuration in Figure 1. The lower section of Figure 1 is the ionosphere above which lies the magnetosphere. At $t = 0$ both of these sections are at rest, but the upper section (magnetosheath) has a velocity V_0. The question is "how does the field and flow evolve for $t > 0$"?

For the moment let us add some simplifying assumptions. Let the ionosphere be perfectly conducting ($\mathbf{E} = 0$), and let the upper section always move with constant speed V_0 (this could occur if the magne-

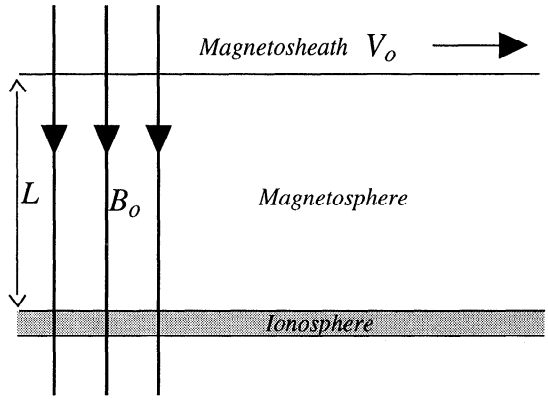

Figure 1. An idealization of recently reconnected field lines. The section of field line in the magnetosphere and ionosphere is initially at rest, while the part in the magnetosheath moves with velocity V_0.

tosheath kinetic energy density far exceeded the other energy densities of the system). Intuitively, we anticipate that the upper part of the field lines will move with speed V_0, while the part of the field lines embedded in the ionosphere will remain at rest ($\mathbf{E} = 0$ in the ionosphere). Thus the field lines in the magnetosphere must be bent over. One final simplification we introduce for the moment is that the timescale of the shearing (L/V_0) be much greater than the period of Alfvén waves (L/V_A; V_A being the magnetospheric Alfvén speed). In subsequent sections we shall relax all these assumptions.

In these circumstances we get a quasi steady state such as that shown in Figure 2a in which the tilt of the field lines (θ) increases with time.

$$\tan\theta(t) = \frac{B_\perp(t)}{B_0} = \frac{V_0 t}{L} \tag{1}$$

At time t, $V_0 t$ is the distance the upper section of the field line has moved, and $\mathbf{B}_\perp$ is the magnetic field induced by the motion. The kink in the field lines of the upper and lower boundaries is associated with a surface current ($j_s = \int j_y dz$) which increases with time

$$j_s = \frac{B_\perp}{\mu_0} = \frac{B_0}{\mu_0}\tan\theta(t) = \frac{B_0 V_0}{\mu_0 L} t \tag{2}$$

It is instructive to study the energy balance of the system. The upper current extracts energy from the "magnetosheath" flow at a rate $\mathbf{V}_0 \cdot \mathbf{j}_s \wedge \mathbf{B}_0$ (equal to $B_0^2 V_0^2 t/\mu_0 L$) per unit area of (x, y). This energy flux per unit area in the $-\hat{\mathbf{z}}$ direction is, of course, equal to the $-\hat{\mathbf{z}}$ component of the Poynting vector evaluated at $z = L$ (i.e., $-\hat{\mathbf{z}} \cdot \mathbf{E} \wedge \mathbf{B}/\mu_0$) and may be confirmed with the aid of (2). The lower surface current does no work since the plasma velocity and electric field are zero there (for an ideal ionosphere). Thus the Poynting flux into the ionosphere vanishes also.

Energy balance may be verified by comparing the energy extracted from the magnetosheath up to a time t with the increased energy stored in the sheared field. The former is

$$\int_0^t \frac{B_0^2 V_0^2}{\mu_0 L} t dt = \frac{B_0^2}{2\mu_0} \cdot \frac{V_0^2 t^2}{L} \tag{3}$$

while the latter (per unit area of (x,y)) is

$$\frac{B_\perp^2(t)}{2\mu_0} L = \frac{B_0^2}{2\mu_0} \cdot \frac{V_0^2 t^2}{L} \tag{4}$$

after recalling (2). Thus the energies and fluxes balance; energy is extracted from the flow and stored in the sheared magnetic field.

For a finite ionospheric Pedersen conductivity (σ_p) the situation is quite different, and the ionospheric surface current is now replaced by a volume current. The induction equation for the ionosphere is

$$\frac{\partial \mathbf{B}}{\partial t} = -\nabla \wedge \mathbf{E} = \nabla \wedge (\mathbf{V} \wedge \mathbf{B}) + \frac{1}{\mu_0 \sigma_p} \nabla^2 \mathbf{B} \tag{5}$$

The first and second terms on the right-hand side give the change in $\mathbf{B}$ due to convection and resistive diffusion, respectively. We may anticipate that as time increases the field threading the ionosphere will become

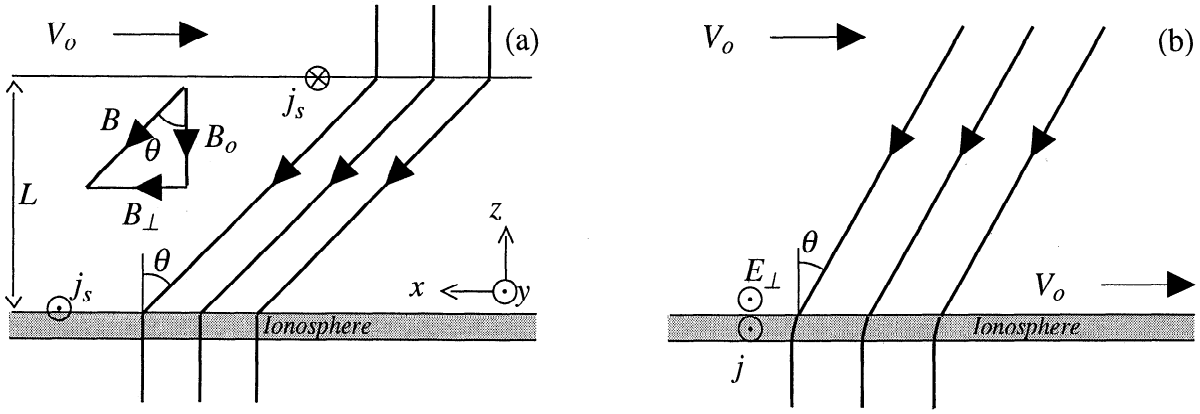

Figure 2. Quasi-steady shearing of magnetospheric field lines when the magnetosheath has constant velocity. (a) For a perfectly conducting ionosphere the field will be tilted indefinitely. (b) When the ionosphere has a finite conductivity the field lines slip and shearing is limited.

more kinked and diffusion will become more important. Ultimately, the field lines will slip through the ionosphere and the entire magnetosphere will move with velocity $\mathbf{V}_0$ (Figure 2b).

We may estimate the time for diffusion to dominate convection by comparing the magnitudes of the convective and diffusive terms in (5). If the ionosphere has a height h, then the convective and diffusive terms are of the order of V_0B_0/h and $B_\perp/(h^2\mu_0\sigma_p)$, respectively. Assuming the ideal convective shear in (1) permits a crude estimate of when diffusion and convection are of a similar order. The two terms are equal when

$$\frac{B_\perp}{B_0} \approx \frac{V_0 t}{L} \approx hV_0\mu_0\sigma_p \equiv R_m \tag{6}$$

(R_m being the ionospheric magnetic Reynold's number).

Hence for $t > \mu_0 L\Sigma_p$ ($\Sigma_p = \sigma_p h$, the height-integrated Pedersen conductivity) the field lines slip, and we have the situation in Figure 2b.

The solution of electric fields and currents in a thin ionosphere has been discussed previously [e.g., *Vasyliunas*, 1970; *Southwood and Hughes*, 1983], and we review the principal properties here. The electric field ($\mathbf{E}_\perp = \hat{\mathbf{y}}E_y$) is constant in a steady state, and in the magnetosphere is produced by convection

$$\mathbf{E}_\perp = -\mathbf{V}_0 \wedge \mathbf{B}_0 \tag{7}$$

In the ionosphere the electric field is associated with the current ($\mathbf{j} = \sigma_p \mathbf{E}_\perp$), which when integrated over the ionosphere's height gives

$$\mathbf{j}_s = \Sigma_p \mathbf{E}_\perp \tag{8}$$

$\mathbf{j}_s$ is the equivalent surface current that is produced by letting the ionosphere become a thin conducting sheet. Writing $\mathbf{j}_s$ in terms of $\mathbf{B}_\perp$ immediately above the ionosphere as in (2) and eliminating $\mathbf{E}_\perp$ with (7), equation (8) yields the ionospheric boundary condition

$$\frac{B_\perp}{\mu_0} = \Sigma_p V_0 B_0 \tag{9}$$

for the fields and flow immediately above the northern ionosphere (at $z = 0^+$). The boundary condition for the southern ionosphere differs from (9) by a minus sign [e.g., *Newton et al.*, 1978]. This boundary condition describes the effect of the ionosphere on the magnetospheric plasma and has been used previously to calculate the decay time of standing Alfvén waves resulting from the dissipative Pedersen currents that are driven in the ionosphere [*Newton et al.*, 1978].

The field lines in the magnetosphere now tilt at an angle θ (Figure 2b),

$$\tan\theta = \frac{B_\perp}{B_0} = \mu_0\Sigma_p V_0 = R_m \tag{10}$$

Energy balance in the new resistive system is quite different from the previous ideal case. Energy is no longer continually stored in the magnetic field but is dissipated in the ionosphere through Joule heating. The Poynting flux per unit area in the magnetosphere directed toward the ionosphere is still

$$-\hat{\mathbf{z}} \cdot (\mathbf{E} \wedge \mathbf{B}/\mu_0) = V_0 B_0 B_\perp/\mu_0 \tag{11}$$

The rate of energy deposition in the ionosphere (per unit area) is

$$\int \frac{1}{\sigma_p} j^2 dz = \int \mathbf{E} \cdot \mathbf{j} dz = V_0^2 B_0^2 \Sigma_p \tag{12}$$

Noting the constraint upon $B_\perp$ in (10), we see that (11) and (12) do indeed balance. Now that we have established the key ideas in magnetosphere/ionosphere coupling we shall refine them in the subsequent sections and begin by considering the time-dependent interaction of the magnetosphere and magnetosheath.

3. Magnetosheath/Magnetosphere Coupling

The idealized steady shearing of open magnetospheric field lines is now replaced by a dynamic, time-dependent description in terms of MHD waves. Consider the flux tube in Figure 3a. It represents the state of the field shortly after reconnection; the lower (magnetosphere) half is at rest, while the upper (magnetosheath) section has a velocity $\mathbf{V}_0$. At $t = 0$ we assume the field line is straight and for simplicity take the density and Alfvén speed to be uniform. How does the system evolve?

A cartoon of the evolved field line is shown in Figure 3b. Physically, the initial jump in velocity breaks down into two propagating Alfvén waves. One propagates up into the magnetosheath and slows the flow down (extracting energy and momentum). The other propagates into the magnetosphere where it speeds up the plasma, increasing the energy and momentum. After a time Δt the sections of tube further away than $V_A\Delta t$ from the discontinuity will be unaware of the boundary and continue in their states of rest or uniform motion. In particular, the upper section has moved a distance $V_0\Delta t$.

Evidently, the sheared section of flux tube in Figure 3b is tilted at an angle θ

$$\tan\theta = \frac{V_0}{2V_A} = \frac{B_\perp}{B_0} \tag{13}$$

and moves with a velocity $V_0/2$. (The distance moved by the center of the flux tube is $V_0\Delta t/2$ in time Δt hence its speed is $V_0/2$.) We see that this description does indeed extract energy from the magnetosheath flow (the speed changes from V_0 to $V_0/2$) while speeding up the magnetospheric plasma (from $V = 0$ to $V_0/2$) over the sections of tube affected by Alfvén waves. It is easy to verify that the energy and momentum lost from the magnetosheath are equal to those gained by the magnetosphere. Here we give the fluxes of these quantities. The $-\hat{\mathbf{z}}$ component of the Poynting vector at the interface is

$$-S_z = \frac{1}{4}\rho_0 V_0^2 V_A \tag{14}$$

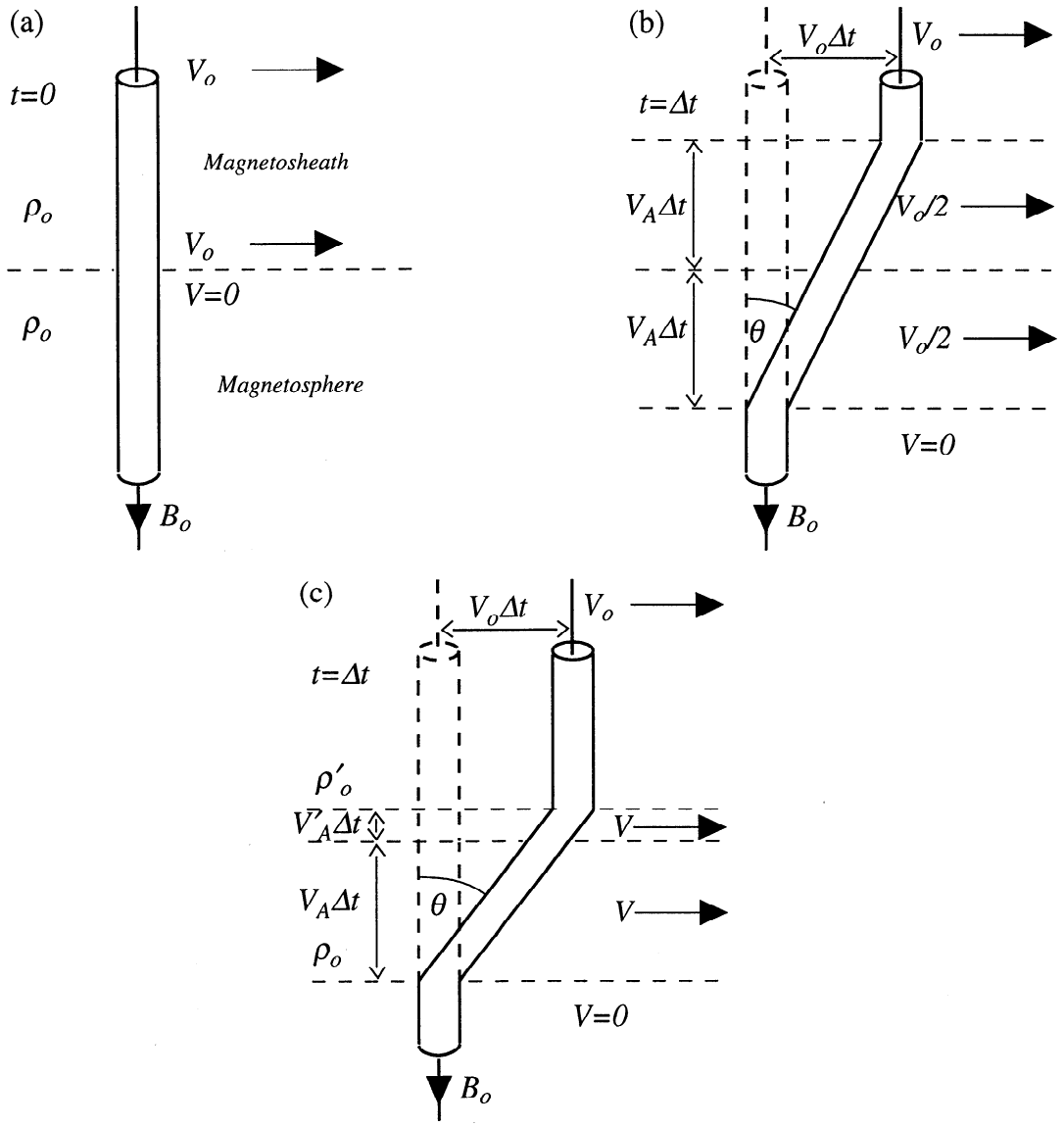

Figure 3. The state of a flux tube embedded in regions with different flow speeds. (a) The state at $t = 0$. (b) The evolved tube at $t = \Delta t$ when the Alfvén speed is constant. (c) The configuration at $t = \Delta t$ when the Alfvén speeds of the two regions are V_A' and V_A and the flow speeds are V_0 and 0, respectively (see section 5 for a discussion of this case).

The momentum flux is soley due to the Maxwell stress for Alfvén waves. The $-\hat{\mathbf{z}}$ component of the flux of $-\hat{\mathbf{x}}$ momentum at the interface is

$$B_0 B_\perp/\mu_0 \equiv \frac{1}{2}\rho_0 V_A V_0 \tag{15}$$

The flux tube shown in Figure 3 may be just one flux element of a much larger open flux tube depending upon the details of reconnection. Each flux element, or field line, can transport energy and momentum in the fashion described above. (In general, the magnetosheath and magnetosphere have different plasma densities and Alfvén speeds. This case is shown in Figure 3c, although we defer discussion of this more complex case until section 5 when some refinements to the basic model are included.)

4. Magnetosphere/Ionosphere Coupling

Ultimately, the Alfvén wave launched into the magnetosphere will encounter the ionosphere where it will suffer some reflection into the magnetosphere and cause the field lines to stop or diffuse through the ionosphere. The diffusion timescale (τ_d) may be estimated from the diffusive term in (5).

$$\frac{B_\perp}{\tau_d} \approx \frac{\partial B_\perp}{\partial t} = \frac{1}{\mu_0\sigma_p}\nabla^2 B_\perp \approx \frac{B_\perp}{\mu_0\sigma_p h^2} \tag{16}$$

(h being the height of the ionosphere). Thus $\tau_d \approx \mu_0\sigma_p h^2 = \mu_0\Sigma_p h$ and for typical ionospheric parameters takes a value of the order of 1 s. Since τ_d is much smaller than typical Alfvén wave periods (hundreds of seconds), we may assume that the ionosphere is always in diffusive equilibrium. Thus the ionosphere may be represented by the boundary condition

$$B_\perp(0^+) = \mu_0\Sigma_p B_0 V(0^+) \tag{17}$$

where $B_\perp(0^+)$ and $V(0^+)$ are the tangential field and flow at $z = 0^+$, that is, immediately above the ionosphere. (Compare with (9) in which we replace V_0 by $V(0^+)$.)

Employing linear ideal MHD in the region above the ionosphere, we find the $\hat{\mathbf{x}}$ component of velocity satisfies the wave equation

$$\frac{\partial^2 V}{\partial t^2} = V_A^2 \frac{\partial^2 V}{\partial z^2} \tag{18}$$

The solution of which is

$$V = f(\phi_1) + g(\phi_2) \tag{19}$$

where $\phi_1(z,t) = z + V_A t$ and $\phi_2(z,t) = z - V_A t$, since the Alfvén speed is uniform in the present model. The component f represents a wave propagating in the $-\hat{\mathbf{z}}$ direction, such as the lower wave in Figure 3b. The g term represents the wave reflected from the ionosphere propagating in the $+\hat{\mathbf{z}}$ direction. The total velocity $(f + g)$ must satisfy the boundary condition (17), and it is this constraint that determines the form of the reflected wave g given the incident wave f. We begin by considering the $\hat{\mathbf{x}}$ component of the induction equation $(z > 0)$

$$\frac{\partial B_\perp(z,t)}{\partial t} = B_0 \frac{\partial V(z,t)}{\partial z} = B_0 \left(\frac{df}{d\phi_1} + \frac{dg}{d\phi_2} \right) \tag{20}$$

(since $\partial\phi_1/\partial z = \partial\phi_2/\partial z = +1$). Integrating (20) with respect to time yields

$$B_\perp(z,t) = B_0 \int \frac{df}{d\phi_1} dt + B_0 \int \frac{dg}{d\phi_2} dt \tag{21}$$

$$B_\perp(z,t) = \frac{B_0}{V_A} f(\phi_1(z,t)) - \frac{B_0}{V_A} g(\phi_2(z,t)) + c(z)$$

since $\partial\phi_1/\partial t = -\partial\phi_2/\partial t = V_A$. The function $c(z)$ is an integration constant and may be determined by initial conditions. For example, let $B_\perp(z > 0, t = 0) = 0$, then (for $z > 0$)

$$c(z) = \frac{B_0}{V_A} \left[g(\phi_2(z,0)) - f(\phi_1(z,0)) \right] \tag{22}$$

We note that the mathematical description developed here is quite general and could be used to generate the evolution shown in Figure 3. In that case, f and g would represent the waves propagating into the magnetosphere and magnetosheath, respectively. It is all a matter of what initial and boundary conditions are imposed. Since the aim of this paper is to develop ideas and concepts useful for describing magnetospheric coupling problems, we presented physical and intuitive arguments to arrive at Figure 3. The interested reader is invited to derive these results more rigorously. The interaction of waves with the ionosphere is not so straightforward, and physical insight may be unreliable. Hence we continue with a more formal analysis of magnetosphere/ionosphere coupling by imposing suitable boundary conditions. Let us suppose that at $t = 0$ no wave has yet been incident upon the ionosphere; $f(\phi_1(z = 0^+, t = 0)) = 0$. If the velocity at $z = 0^+$ is also zero, (19) tells us that, of course, there is no reflected wave there either; $g(\phi_2(z = 0^+, t = 0)) = 0$. These conditions require $c(z = 0^+) = 0$ from (22), and (21) implies $B_\perp(z = 0^+, t = 0) = 0$ also. Now let us impose the boundary condition (17) at $z = 0^+$, but for $t > 0$. Substituting (19) and (21) into (17) with the above assumptions gives

$$\frac{B_0}{V_A} \left[f(\phi_1(0^+,t)) - g(\phi_2(0^+,t)) \right] = \mu_0\Sigma_p B_0 \left[f(\phi_1(0^+,t)) + g(\phi_2(0^+,t)) \right] \tag{23}$$

and on rearrangement yields the reflected wave in terms of the incident wave;

$$g(\phi_2(0^+,t)) = \beta f(\phi_1(0^+,t)) \qquad \beta = \frac{1 - \mu_0\Sigma_p V_A}{1 + \mu_0\Sigma_p V_A} \tag{24}$$

The reflection coefficient β was first derived by *Scholer* [1970], who considered the pattern of Alfvén waves that could become established from multiple reflections between the ionospheric end points of closed field lines. Here we have generalized the derivation by considering arbitrary initial conditions (through the function $c(z)$).

We can recover several familiar results from (24): For a perfectly conducting ionosphere ($\Sigma_p \to \infty$), $\beta \to -1$, and the reflected velocity (g) is equal and opposite to the incident velocity (f). For a perfectly insulating ionosphere ($\Sigma_p \to 0$), $\beta = 1$. For a finite Σ_p, $|\beta| < 1$, and we have partial reflection of the incident wave. For the special case of an impedance matched ionosphere ($\Sigma_p = 1/(\mu_0 V_A)$) the incident wave is completely absorbed and there is no reflected wave, $\beta = 0$ [e.g., *Southwood and Hughes*, 1983].

We are now in a position to extend the system depicted in Figure 3 by including an encounter with the ionosphere. The new evolution of the magnetic field is shown in Figure 4a for $\Sigma_p \to \infty$. At $t = 0$ the field line is straight. At $t = t_1$ the field line is bent in a configuration identical to that in Figure 3b (the ionosphere has not yet been encountered by the waves). A dashed (upper) characteristic is shown inclined at the Alfvén Mach number ($\tan\theta_A = V_0/V_A = M_A$) and originating from the magnetopause. Above this characteristic the plasma has a speed V_0. At $t = t_1$ the wave launched into the magnetosphere has only propagated halfway down to the ionosphere and has tilted the field at an angle θ

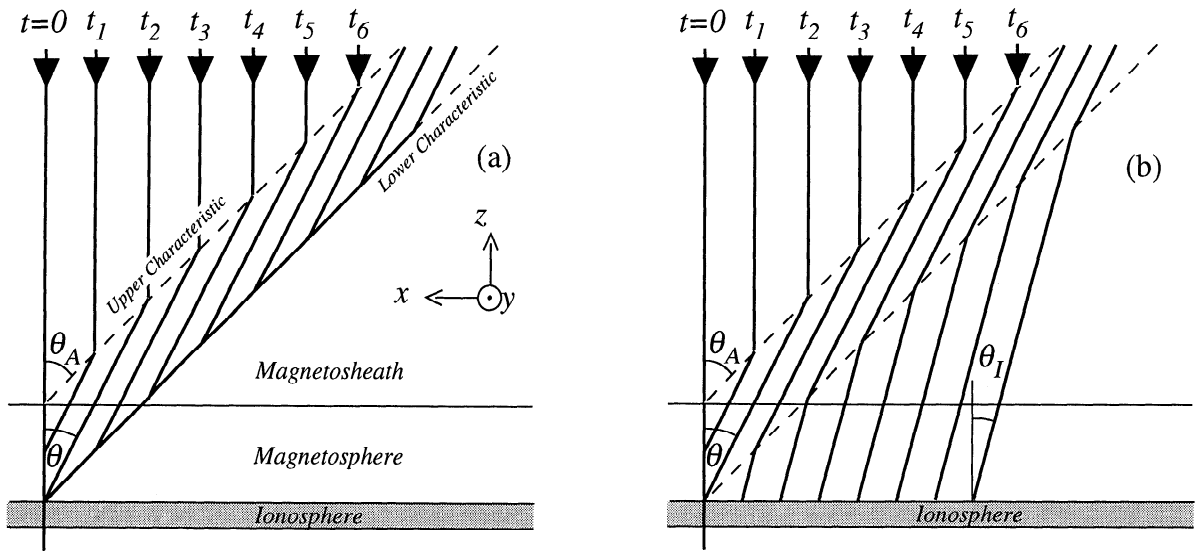

Figure 4. Superposed snapshots of the state of a field line at successive times. Waves propagate along the characteristics indicated. (a) When $\Sigma_p = \infty$, the ionosphere completely arrests the field line, which ultimately aligns itself with the lower characteristic. (b) When $\Sigma_p \neq \infty$, the field line is able to slip relative to the ionosphere.

(the same as in Figure 3b and (13)). At $t = t_2$, the wave has just reached the ionosphere, and we expect that a reflected Alfvén wave will be launched from the ionosphere. The lower characteristic (also inclined at θ_A) denotes the trajectory of this reflected wave. At $t = t_3$ the field line has three distinct sections. The untitled section above the upper characteristic is unperturbed and moves with speed V_0. The middle section (between the two characteristics) is inclined at an angle θ and moves with speed $V_0/2$. The lower section is tilted at θ_A and coincides with the lower characteristic. The latter section has zero velocity and is a result of $\Sigma_p \to \infty$; the velocity of the reflected wave is equal and opposite to the incident wave, thus arresting the flux tube. For $t = t_3$ and later times the solution corresponds to two waves propagating in the $+\hat{\mathbf{z}}$ direction (one from the magnetopause and the other reflected from the ionosphere). As t increases from t_4 to t_6 we see kinks propagate along $+\hat{\mathbf{z}}$. Energy is being extracted from the magnetosheath at the rate given in (14). However, as most of the perturbed section of field line (particularly at later times) is at rest, the energy is stored in shearing the magnetic field to an angle θ_A. The momentum flux from the magnetosheath is directed into the ionosphere for $t > t_4$ (since the magnetosphere section of field line is at rest). The flux is twice that given on the right-hand side of (15) as $B_\perp(0^+)/B_0 = V_0/V_A$ for $t > t_4$. (Although the momentum of the ionosphere increases, we assume it is sufficiently massive that it does not aquire a significant velocity.)

Figure 4b shows the evolution of a field line when $\Sigma_p \neq \infty$. For $t \leq t_2$ the waves have not encountered the ionosphere, and the evolution is identical to that in Figure 4a. For $t > t_2$ the solution is determined by the wave reflected from the ionosphere, the amplitude of which is determined by (24). When $\Sigma_p \neq \infty$ or 0, $|\beta| < 1$. For typical ionospheric and magnetospheric parameters β will be negative, and Figure 4b depicts this situation ($-1 < \beta < 0$, i.e., $1/(\mu_0 V_A) < \Sigma_p < \infty$). The net effect is that the reflected wave is not large enough to arrest the magnetospheric flow, which moves with a speed equal to the sum of the incident plus reflected wave velocities;

$$V(0^+) = \frac{V_0}{2}(1+\beta) = \frac{V_0}{1+\mu_0\Sigma_p V_A} \tag{25}$$

Thus field lines entering the ionosphere are now tilted at an angle θ_I given by (using (17))

$$\tan\theta_I = \frac{B_\perp(0^+)}{B_0} = \mu_0\Sigma_p V(0^+) \equiv \frac{\mu_0\Sigma_p V_0}{1+\mu_0\Sigma_p V_A} \tag{26}$$

This is a general result, and recovers two familiar limits. (1) $\Sigma_p \to \infty$; $\beta \to -1$; and $\tan(\theta_I) \to V_0/V_A$, that is, $\theta_I \to \theta_A$, as in Figure 4a. (2) $\Sigma_p \to 0$; $\beta \to +1$; and $\tan\theta_I \to 0$, that is, $\theta_I \to 0$, a perfectly insulating boundary condition.

An alternative way of viewing the finite $V(0^+)$ when $\Sigma_p \neq \infty$ is to envisage the field diffusing or slipping through the resistive ionosphere. $V(0^+)$ is the velocity with which the field lines slip. A crude estimate of this velocity can be found from taking $V_A \sim 10^7$ m/s (above the ionosphere) and $\Sigma_p = 10$ mho, giving $1/(\mu_0\Sigma_p V_A + 1) \approx 0.01$. Thus the flow above the ionosphere is of the order of 1% of the sheath flow speed (V_0). Taking V_0 to be typically 250 km/s suggests an F region flow speed of 2.5 km/s. Of course, this simple calculation assumes that all of the earthward propagating Alfvén wave reaches the ionosphere. In reality, the nonuniformities in B_0 and ρ_0 will cause some of this wave to be reflected from the body of the magnetosphere itself.

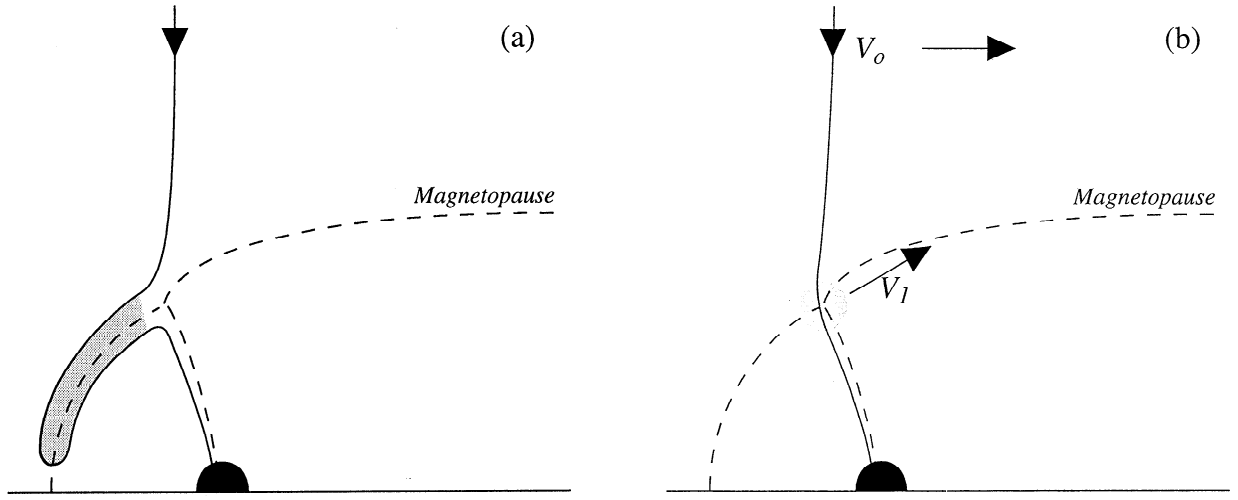

Figure 5. The state of a field line immediately after being reconnected (solid line). The dotted lines represent the northern magnetopause and cusp, while the black disc represents the Earth. (a) The shaded area of plasma will be accelerated until the field line is straight (b) at which point it has a speed (V_1) of the order of the Alfvén speed.

The wave model of the interaction of a background flow with a load has been considered previously in space plasmas. In the present study the load is represented by a magnetosphere that is initially at rest and a resistive ionosphere. In other related studies the load has been an artificial satellite [*Drell et al.*, 1965; *Scholer*, 1970] or the jovian satellite Io, [e.g., *Neubauer*, 1980; *Southwood et al.*, 1980; *Wright and Southwood*, 1987]. Indeed, the sketches of the interaction of Io with the jovian magnetosphere bear a striking resemblance to Figure 4 when $\Sigma_p = \theta_I = 0$.

5. Magnetopause Flows

The one-dimensional model developed so far can easily be extended to include effects such as the accelerated magnetopause flow that is associated with reconnection [e.g., *Sonnerup et al.*, 1981; *Paschmann et al.*, 1985]. Consider the newly reconnected field line shown in Figure 5a. As the field line relaxes under field line tension, the volume of plasma shown as the shaded region will be accelerated up to around the local Alfvén speed. Figure 5b depicts the state after relaxation, and Figure 6 displays the one-dimensional model that may mimic this state. The accelerated plasma may be thought of as having an enhanced velocity (V_1) over a section of the tube close to the magnetopause. In our model (Figure 6) we represent this as a slab of plasma separating the magnetosheath and magnetosphere ($z_1 < z < z_2$). Assuming for the moment that the density throughout the system is constant, we can derive the flow speed that would be observed in the F region ($z = 0^+$). Now we have two discontinuitites in tangential velocity at $t = 0$, where $z = z_1$ and $z = z_2$. Both discontinuities will launch Alfvén waves in the way described previously. A little thought gives the resulting flow in Figure 7a; at $t = z_1/V_A$ the Alfvén wave initiated from $z = z_1$ reaches the ionosphere, and the flow jumps to $V_{\max} = V_1/(1 + \mu_0\Sigma_p V_A)$. A short time later (at $t = z_2/V_A$) the Alfvén wave launched from z_2 reaches the ionosphere, and the flow is reduced to $V_\infty = V_0/(1+\mu_0\Sigma_p V_A)$. Thus the net effect of the accelerated magnetopause flow is to produce an intital surge in the ionospheric flow. The interested reader may like to sketch figures similar to Figure 4 for the new model in Figure 6.

The model can be made more realistic by allowing for the fact that the Alfvén speed varies along the field lines from the magnetosphere through the magnetopause flow and into the sheath. If we assume that the density between z_1 and z_2 is much greater than elsewhere, we shall have a situation similar to that in Figure 2 where the field lines are sheared indefinitely (unless $\Sigma_p \neq \infty$). In terms of waves, this behavior results from

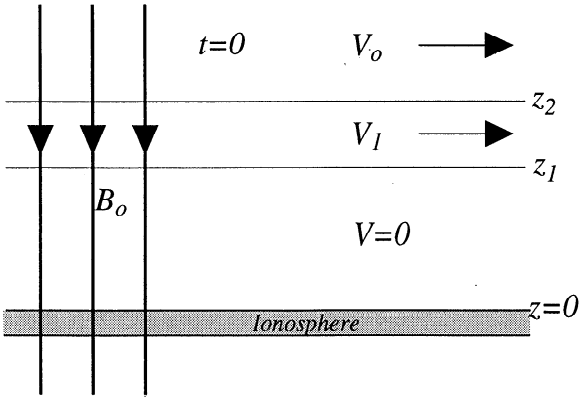

Figure 6. A model of the situation in Figure 5b: The accelerated flow is included as a layer (z_1 to z_2) moving with speed V_1 separating the stationary magnetosphere and flowing magnetosheath (V_0).

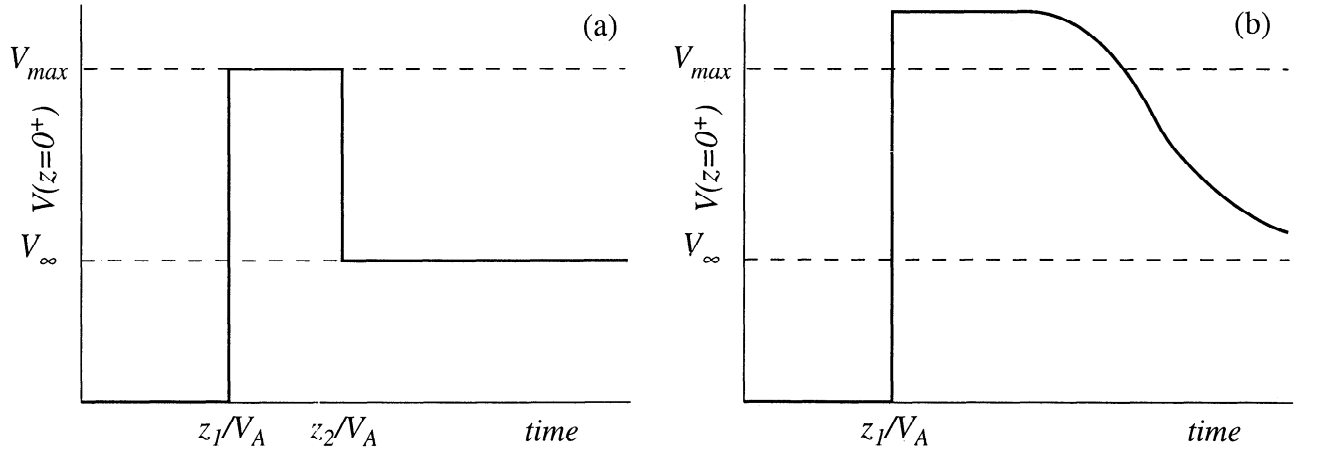

Figure 7. The response produced at $z = 0^+$ (i.e., immediately above the ionosphere) by the initial condition sketched in Figure 6. (a) When the Alfvén speed is taken to be constant there is an initial surge of flow to $V_{\max} = V_1/(1+\mu_0\Sigma_p V_A)$ which steps down to $V_\infty = V_0/(1+\mu_0\Sigma_p V_A)$. (b) If the Alfvén speed of the accelerated flow is smaller than that in the magnetosphere, the surge will exceed $V_{\max}$ and then decay to V_∞.

the changes in V_A (i.e., ρ_0) producing reflection and transmission of the intital Alfvén waves launched from the velocity discontinuities. For example, the earthward wave from z_1 suffers partial reflection from the ionosphere and propagates back to $z = z_1$. At this point the wave is partially reflected and transmitted, and the new reflected wave causes the magnetospheric field to tilt more than in the previous constant V_A and ρ_0 case. Of course, the discontinuity in density at $z = z_2$ will also give rise to reflection and transmission of waves.

To understand the full effect of a discontinuity in Alfvén speed, we return to Figure 3 and consider a velocity discontinuity that is also a discontinuity in V_A or ρ. The system will not evolve to the state shown in Figure 3b but to that in Figure 3c when the jump in velocity is from V_0 to 0 and that in density from ρ_0' to ρ_0. The corresponding change in Alfvén speed is from V_A' to V_A. The tube is now tilted at an angle θ

$$\tan\theta = \frac{B_\perp}{B_0} = \frac{V_0}{V_A + V_A'} \tag{27}$$

since the waves propagate different distances away from the discontinuity. The speed of the tilted section is given by

$$V = V_0 \cdot \frac{V_A}{V_A + V_A'} \tag{28}$$

and it is easy to verify that this solution conserves energy and momentum by the analysis used previously. Once again, energy and momentum are transferred from the moving layer to the stationary plasma. The $-\hat{\mathbf{z}}$ component of the energy flux (Poynting flux) per unit area at the discontinuity is

$$-S_z = \rho_0 V_0^2 V_A \left(\frac{V_A}{V_A + V_A'}\right)^2 \tag{29}$$

whilst the $-\hat{\mathbf{z}}$ component of the flux of $-\hat{\mathbf{x}}$ momentum density is

$$B_0 B_\perp/\mu_0 \equiv \rho_0 V_0 V_A \left(\frac{V_A}{V_A + V_A'}\right) \tag{30}$$

The fluxes are generalizations of those derived in (14) and (15) which were for the limit $\rho_0' = \rho_0$ and $V_A' = V_A$.

With these results we can now calculate the variation of $V(0^+)$ for an enhanced density between z_1 and z_2 (see Figure 7b). Two features to note are the "overshoot" of $V_{\max}$ and the decay rather than jump to V_∞. The latter property may be appreciated by thinking of the wave reflected from the ionosphere as being trapped in the magnetosphere and having to leak through the discontinuities in density. Note that the limit ρ'/ρ and $V_A/V_A' >> 1$ (which corresponds to perfect reflection of magnetospheric waves incident upon the density dicontinuity) is the situation considered by *Kan and Sun* [1985]. In this case the continual reflections tilt the magnetic field indefinitely until balanced by ionospheric footpoint slippage.

The origin of the overshoot in Figure 7b is now clear; from (28) we see that if $V_0 = V_1$ and $V_A' = V_A$, then the amplitude of the Alfvén wave launched toward the ionosphere is $V_1/2$. However, when $V_A' < V_A$, the Alfvén wave propagating toward the ionosphere will have a larger amplitude (from (28)), and thus $V(0^+)$ exceeds its former value.

If we are not concerned with transient flow bursts but rather the efficiency with which magnetosheath energy and momentum may be supplied to the magnetosphere on larger timescales, then taking V_A and V_A' to represent the Alfvén speeds in these regions enables us to estimate the fluxes of these quantities from (29) and (30).

6. Ionospheric Flow Patterns

The ionospheric flow resulting from dayside reconnection is sensitive to the IMF B_y component [e.g., *Lockwood et al.*, 1995]. Observations show that dayside reconnection causes the polar cap boundary to ex-

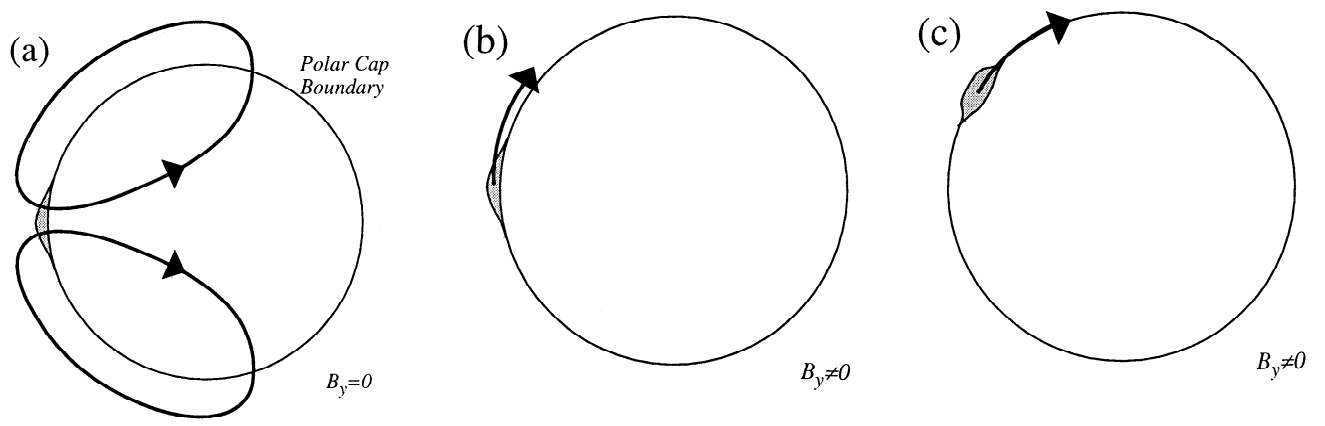

Figure 8. The ionospheric flows (solid arrows) produced by newly reconnected flux. (a) When $B_y = 0$, the reconnected flux eventually piles up against the existing polar cap flux and thereafter contributes to the large-scale convection pattern. (b) When $B_y \neq 0$, the flux tends to move azimuthally "between the sheets" of existing open and closed flux and evolves to the state shown in (c).

pand equatorward as more open flux is added to the polar cap flux [*Lockwood et al.*, 1990a]. Figure 8a shows the polar cap boundary and an equatorward region (shaded grey) representing the footpoints of newly opened field lines. If $B_y = 0$, the field lines reconnected at the subsolar point will be confined (approximately) to the moon-midnight meridian. They will move antisunward and pile up against the existing open flux. Clearly, this situation is two-dimensional, and our one-dimensional wave model will have limited validity here. We may expect the initial "pre-pile-up" phase to be described by the wave model. Thereafter the newly opened flux simply adds to the body of existing open flux and contributes to the large-scale ionospheric convection pattern (shown by the arrows in Figure 8a). We can, of course, think of all the open flux extracting momentum and energy from the magnetosheath, although the quasi-stationary cartoon in Figure 2 may describe the ionospheric end better than a wave description, which may suit the magnetosheath more.

When $B_y \neq 0$, a significant tension force acts to move the newly reconnected field lines azimuthally rather than poleward, and is depicted in Figure 8b [*Lockwood et al.*, 1990b]. The reconnected flux finds it difficult to move poleward or equatorward as this will require displacing open or closed field lines, respectively. Indeed, when viewed from the pole one can envisage the polar cap boundary as the discontinuity between the last sheet of open polar cap flux and the first sheet of closed magnetospheric flux. The (relatively) unimpeded route for the newly reconnected flux is to slip "between the sheets," that is, move azimuthally away from noon to the state depicted in Figure 8c. We may anticipate that this type of motion may be well-approximated by our one-dimensional model as there is no flux pile-up. Indeed, it is noteworthy that the flows with an initial surge seem to be observed preferentially when $B_y \neq 0$, and are directed predominantly azimuthally [*Lockwood et al.*, 1990b, 1995]. Once the azimuthal tension force has been expended the footpoint motion slows and reverts to a more poleward direction in keeping with the background convection pattern.

7. Summary

In an effort to emphaisise the dynamical nature of magnetosheath/magnetosphere/ionosphere coupling we have developed a simple wave model for this problem. The description of the magnetosheath/magnetosphere interaction is novel and yields analytical expressions for the rate at which energy and momentum are extracted from the magnetosheath flow. The preliminary study here offers an alternative view to steady state analyses and, we hope, will serve as a springboard for future time-dependent studies. Such work should address the two-dimensional "flux pile-up" effects that become important when $B_y = 0$. Other refinements include a detailed study of how Alfvén waves launched from the magnetopause will propagate along magnetospheric field lines for realistic variations in field strength and density.

Acknowledgments. This work was carried out while the author was supported by a UK PPARC Advanced Fellowship. Discussions with M. P. Freeman and M. Lockwood are gratefully acknowledged.

The Editor thanks W. Jeffrey Hughes and another referee for their assistance in evaluating this paper.

References

Drell, S. D., H. M. Foley, and M. A. Ruderman, Drag and propulsion of large satellites in the ionosphere, *J. Geophys. Res., 70,* 3131, 1965.

Ellis, P., and D. J. Southwood, Reflection of Alfvén waves by nonuniform ionospheres, *Planet. Space Sci., 31,* 107, 1983.

Glassmeier, K. H., Comment on "A transient response model of Pi 2 pulsations" by J. R. Kan, D. U. Longenecker, and J. V. Olsen, *J. Geophys. Res., 88,* 7261, 1983.

Glassmeier, K. H., Reconstruction of the ionospheric influence on ground-based observations of a short duration ULF pulsation event, *Planet. Space Sci., 36,* 801, 1988.

Glassmeier, K. H., Traveling magnetospheric convection twin-vorticies: Observations and theory, *Ann. Geophys., 10,* 547, 1992.

Holzer, T. E., and G. C. Reid, The response of the day side magnetosphere-ionosphere system to time-varying field line reconnection at the magnetopause, 1, Theoretical model, *J. Geophys. Res., 80,* 2041, 1975.

Hughes, W. J., Hydromagnetic waves in the magnetosphere, in *Solar-Terrestrial Physics,* edited by R. L. Carovillano and J. M. Forbes, D. Reidel, Norwell, Mass., 1983.

Kan, J. R., and W. Sun, Simulation of the westward traveling surge and Pi 2 pulsations during substorms, *J. Geophys. Res., 90,* 10,911, 1985.

Kan, J. R., D. U. Longenecker, and J. V. Olsen, A transient response model of Pi 2 pulsations, *J. Geophys. Res., 87,* 7483, 1982.

Lockwood, M., S. W. H. Cowley, and M. P. Freeman, The excitation of plasma convection in the high latitude ionosphere, *J. Geophys. Res., 95,* 7961, 1990a.

Lockwood, M., S. W. H. Cowley, P. E. Sandholt, and R. P. Lepping, The ionospheric signatures of flux transfer events and solar wind dynamic pressure changes, *J. Geophys. Res., 95,* 17,113, 1990b.

Lockwood, M., S. W. H. Cowley, P. E. Sandholt, and U. P. Lovhaug, Causes of plasma flow bursts and dayside auroral transients: An evaluation of two models invoking reconnection pulses and changes in the Y component of the magnetosheath field, *J. Geophys. Res., 100,* 7613, 1995.

Maltsev, Y. P., W. B. Lyatsky, and A. M. Lyatskaya, Currents over the auroral arc, *Planet. Space Sci., 25,* 53, 1977.

Neubauer, F. M., Nonlinear Standing Alfvén wave current system at Io: Theory, *J. Geophys. Res., 85,* 1171, 1980.

Newton, R. S., D. J. Southwood, and W. J. Hughes, Damping of geomagnetic pulsations by the ionosphere, *Planet. Space Sci., 26,* 201, 1978.

Paschmann, G., I. Papamastorakis, N. Sckope, B. U. Ö. Sonnerup, S. J. Bame, and C. T. Russell, ISEE observations of the magnetopause: Reconnection and energy balance, *J. Geophys. Res., 90,* 12,111, 1985.

Scholer, M., On the motion of artificial ion clouds in the magnetosphere, *Planet. Space Sci., 18,* 977, 1970.

Sonnerup, B. U. Ö., G. Paschmann, I. Papamastorakis, N. Sckope, G. Haerendel, S. J. Bame, J. R. Asbridge, J. T. Gosling, and C. T. Russell, Evidence for magnetic field reconnection at the Earth's magnetopause, *J. Geophys. Res., 86,* 10,049, 1981.

Southwood, D. J., M. G. Kivelson, R. J. Walker, and J. A. Slavin, Io and its plasma environment, *J. Geophys. Res., 85,* 5959, 1980.

Southwood, D. J., The ionospheric signature of flux transfer events, *J. Geophys. Res., 92,* 3207, 1987.

Southwood, D. J., and W. J. Hughes, Theory of hydromagnetic waves in the magnetosphere, *Space Sci. Rev., 35,* 301, 1983.

Vasyliunas, V. T., in *Particles and Fields in the Magnetosphere,* edited by B. M. McCormac, p. 60, D. Reidel, Norwell, Mass., 1970.

Wright, A. N., and D. J. Southwood, Stationary Alfvénic Structures, *J. Geophys. Res., 92,* 1167, 1987.

Yarker, J. M., and D. J. Southwood, The effect of nonuniform ionospheric conductivity on standing magnettospheric Alfvén waves, *Planet. Space Sci., 34,* 1213, 1986.

A. N. Wright, Mathematical Institute, University of St. Andrews, St. Andrews, Fife KY16 9SS, Scotland, U.K. (e-mail: andy@dcs.st-and.ac.uk)

(Received August 24, 1995; revised December 5, 1995; accepted February 12, 1996.)